Computing and Informatics, Vol. 44, 2025, 366–384, doi: 10.31577/cai_2025_2_366

MAX PLANCK THEORY FOR DIGITAL IMAGE PROCESSING: A NEW ALGORITHM FOR MAMMOGRAM IMAGE SEGMENTATION TO IDENTIFY MASSES IN REGIONS OF THE BREAST

Yun Zhang[§]

Gaomi Maternity and Child Healthcare Hospital
Shandong Province, 261500, China

Refat Mohammed Abdullah Eshaq[§]

Mechanical Engineering Department, Faculty of Science and Engineering
Swansea University, SA1 8EN, UK

Weian Dong

College of Mechanical and Electrical Engineering, Hohai University
Changzhou 213022, China

Chunxu Li*

Mechanical Engineering Department, Faculty of Science and Engineering
Swansea University, SA1 8EN, UK
e-mail: chunxu.li@swansea.ac.uk

Abstract. Breast cancer, per WHO, ranks top in diagnoses and cancer fatalities. Early detection via mammography reduces mortality significantly, yet mammogram

§ Co-first authors
* Corresponding author

images often have indistinct features. Hence, precise tumor edge identification requires both image enhancement and segmentation. In response, we introduce the Max Planck Algorithm, a novel segmentation method rooted in Planck's quantum theory, specifically his thermal radiation principles. We innovatively converted this theory to create a unique segmentation tool applicable to digital image processing and medical imaging. The algorithm works by relating mammogram pixel values to X-ray wavelengths, adapting Planck's Law to use 'temperature' as an arbitrary variable (originally tied to actual temperature in Planck's work). Gradually adjusting 'temperature' optimizes the mammogram image's meaningfulness. The Max Planck Algorithm boasts advantageous properties, delivering higher efficiency and superior segmentation results. This innovative model introduces new methods for enhancing and segmenting mammograms, establishing itself as a unique technique without comparison to existing methods.

Keywords: Image processing, computer vision, pattern recognition, image segmentation, Max-Planck theory, mammogram image

1 INTRODUCTION

Digital image processing has become an integral part of most applications, and it is making major advances in solving problems of image filtering, image restoration, image reconstruction, color image processing, image transforms, image compression, morphological image processing, image segmentation, feature extraction, and image pattern classification. Recently, a new technology emerged, called deep learning (DL), a subset of machine learning, and have proved its capability to solve certain problems in image processing such as image classification, object detection, and image segmentation; nevertheless, this technology suffers from intense several negative effects. We think that deep learning will reach to saturation state, which means, there will not be many more successes in the near future because it requires a very powerful GPU. Both image processing and deep learning are affected by three factors: first, the development of computers; second, the development of mathematics; third, the demand for a wide range of applications has tremendously increased in medical science, agriculture, industry, environment, and military.

Since the emergence of digital image processing in the 1960s, most computer scientists have focused on techniques inspired by mathematical and evolutionary theories to create algorithms for image processing and deep learning; however, they completely neglected the physical theories and the effects of physics on image processing and deep learning. This aspect prompted us to focus in depth on adding a new concept inspired by physical theories, namely Planck's law of quantum theory, to the digital image processing industry, especially image segmentation.

Image segmentation is one of the fundamental approaches of digital image processing and analysis, and it is the foundation of computer vision. The main purpose of the utilization of image segmentation is to partition an image into multiple parts or regions, often based on the characteristics of the pixels in the image. Image segmentation is frequently used in medical imaging to identify and label picture pixels in a patient's organs. Segmentation in mammography is a critical process for isolating regions of interest, such as potential tumors or anomalous areas. By precisely delineating these regions, segmentation enables radiologists to conduct a more thorough analysis of abnormalities, enhancing diagnostic accuracy. It facilitates the detection of early-stage tumors that may be overlooked in unprocessed images, thereby significantly improving early diagnosis, which is crucial for effective treatment and better survival rates. Furthermore, segmentation provides quantitative measurements of tumor attributes, including size and shape. These metrics are instrumental in monitoring disease progression and devising tailored treatment strategies.

The development of image segmentation algorithms, as shown in Figure 1, is classified into three main categories: traditional methods, such as edge detection (Robert Operator-Based Edge Detector [1], Sobel Operator-Based Edge Detector [2], Kirsch Operator [3], Laplacian and Difference of Gaussian-Based Edge Detector [4], Canny's Edge Detector [5]), thresholding [6], histogram-based bundling, region growing [7], k-means clustering [8], watersheds [9]; the more advanced techniques such as active contours [10], graph cuts [11], conditional and Markov random fields [12], and sparsity based [13, 14] methods; and deep learning-based segmentation (DLS) methods. For more information on the recent literature in image segmentation using deep learning techniques, we refer our reader to [15].

Undoubtedly, the performance of deep learning-based segmentation (DLS) has surpassed most traditional image segmentation algorithms and has been reported to yield remarkable improvements for several difficult segmentation problems, similar to deep convolutional neural networks (CNNs) [16, 17] that are used for image classification, object detection, and scene parsing [18]. DLS excels at identifying and extracting features from medical images that may be challenging for human radiologists to discern. However, the reliance on these techniques in critical fields, such as medicine or industry, has potentially serious consequences.

Both DLS and CNNs were designed to deal with sets of object categories (e.g., human, animal, insect, vehicle, tree, flower, sky, appliance) [19]. Scholars and researchers in computer science, however, do not generally have a basic knowledge of biological and physical phenomena; therefore, how can the algorithms created for those phenomena be authenticated? Technically, the traditional layers of CNNs such as convolutional layers, nonlinear activation functions layers, batch normalization layers, and polling layers, destroy the images, which causes several negative effects (e.g., losing background information, foreground texture information, missing significant data patterns, etc.). Moreover, DLS and CNNs require powerful GPUs and a large number of images to obtain the best generalization (referred to as the big data problem). Regardless of the high accuracy of DLS and CNNs, the adoption of these techniques in the medical field or industry fields is still questionable and challenging because those techniques were built based on simple mathematical calculation. Moreover, from a methodology perspective, DLS and CNNs are a simple combination of convolutional layers, nonlinear

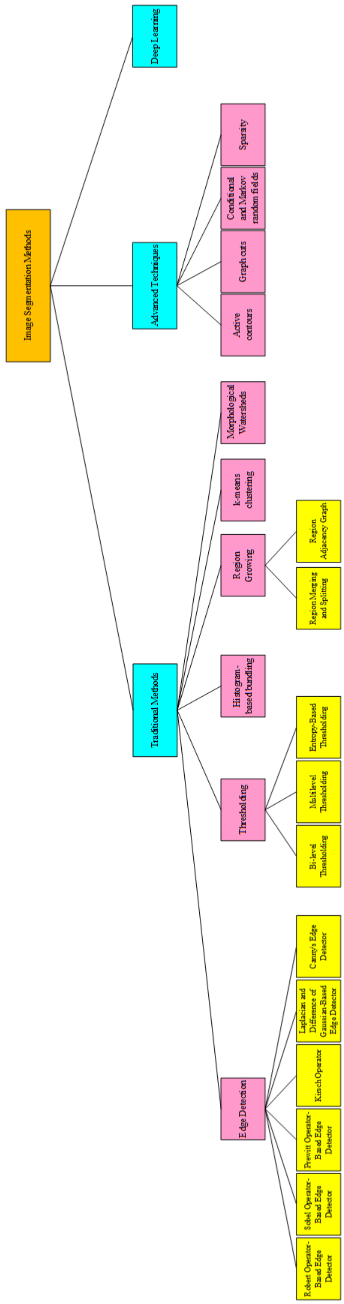

Figure 1. The development of image segmentation over the history

activation functions layers, batch normalization layers, polling layers, and dropout layers, which bring up many questions about their effectiveness in other different fields.

In this article, a novel algorithm for image segmentation is proposed, namely, the Max Planck algorithm. This algorithm works based on the famous quantum theory by scientist Max Planck. The method appears simple, but it is powerful in the field of medical imaging, particularly in the use of mammogram images of breast cancer to study the shape of both benign and malignant masses that form in the breast. Mammography was developed based on X-ray imaging to generate high-resolution images. When X-rays pass through the organ (breast), different tumors absorb the energy at different rates. A detector that picks up the X-rays after they have passed through the breast turns them into an X-ray image. Pixels of the X-ray image are inversely proportional to photon energy. Likewise, the wavelength of the X-rays is inversely proportional to photon energy. This similarity between pixel and wavelength provided the motivation to utilize the concept of quantum theory for image segmentation. According to our investigation, this method has never been applied in the field of computer science (see [20, 21, 22, 23, 24, 25]). Hence, we advanced the research further by creating a new algorithm for image segmentation. In summary, this article's major contributions are threefold as follows:

1. A novel image segmentation algorithm using the Max Planck's theory is proposed. To the best of my knowledge, we are the first to use the Max Planck's theory in image segmentation. Therefore, this is the first exploration of the potential of Max Planck's theory for image segmentation tasks.
2. The method was evaluated on mammogram images of breast cancer. The results indicate that the proposed algorithm produces successful results in detecting the cancerous regions. Each pixel of the breast tissue can be categorized as intact cells, masses, or irregular tissue. The Max Planck algorithm was used in X-ray imaging for medical purposes because this imaging method is based on quantum theory.
3. It is important to note that the proposed Max Planck algorithm is simple; however, the question remains as to why scholars and researchers in computer science have not discovered or applied this solution before. This article therefore carries an appealing letter to the scientific community to research beyond DLS and CNNs. Physics has its own logic and concepts, and it is completely independent of mathematics, meaning it has unparalleled opportunities.

2 BACKGROUND

2.1 Mammography

Since the discovery of X-rays on November 8, 1895 by German physics Professor Wilhelm Röntgen [26], the popularity of the X-ray machine has grown tremendously, especially in the medical field. Mammography is a type of X-ray used to examine the breasts. For many women, mammography is a highly effective means of detecting early stage breast cancer because it has been demonstrated that mortality can be significantly reduced if the disease is detected at an early stage [27] (the credit is largely owed to Professor Wilhelm Röntgen). When the X-rays pass through the breast, as shown in Figure 2, the pixel value $x_{i,j}$ and photon energy (E) are inversely proportional. A breast tumor has high density, which means it absorbs the photon energy of X radiation. As a result, the tumor region appears to be lighter than the normal area. To clarify, in a gray-scale image, each pixel $x_{i,j}$ has a value between 0 and 255, where zero corresponds to "black" and 255 corresponds to "white". The values in between 0 and 255 are varying shades of gray, where values closer to 0 are darker and values closer to 255 are lighter [28]. Simply, this phenomenon can be expressed based on our observation as follows:

$$x_{i,j} \propto \frac{1}{E}. \tag{1}$$

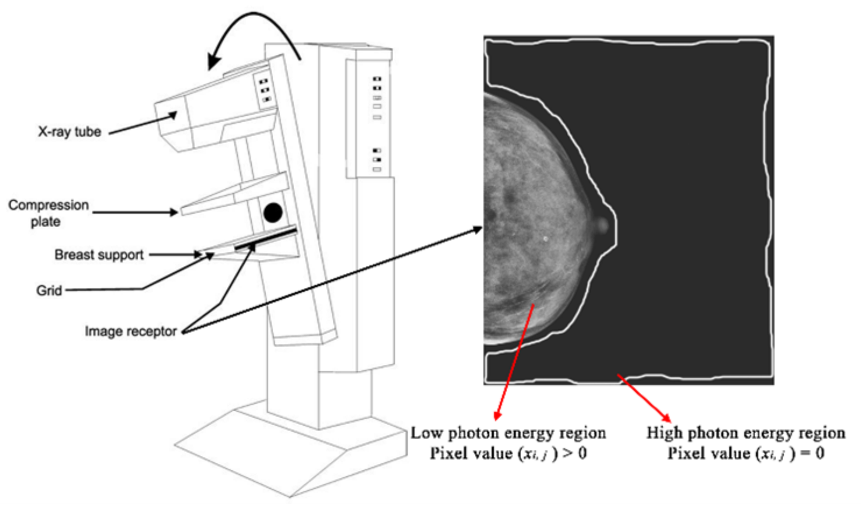

Figure 2. The process of capturing mammogram images of the breast [27, 28, 29, 30, 31, 32, 33]

2.2 Theory of Thermal Radiation

In 1900, German physics Professor Max Planck proposed that electromagnetic radiation is the propagation of a collection of discrete packets of energy called photons or quanta [29, 30]. Based on this perspective, each photon of frequency v is considered to have an energy of:

$$E = hv = h\frac{\tau_0}{\lambda}, \tag{2}$$

where E is the radiant energy or photon energy, $h = 6.62607015 \times 10^{-34}\,\mathrm{J \cdot s}$ is Planck's constant, v is the frequency of the electromagnetic wave, λ is the wavelength, and τ_0 is the speed of light. It is known that the relationship between frequency and wavelength are inversely proportional. Therefore, Equation (2) can be written as:

$$\lambda = h\frac{\tau_0}{E}. \tag{3}$$

From Equation (3), we deduce that λ is inversely proportional to photon energy, which is nearly the same as the behaviour of the pixel value (see Equation (1)). Therefore, we can also express the relationship between wavelength and photon energy as follows:

$$\lambda \propto \frac{1}{E}. \tag{4}$$

The relation for the spectral black-body emissive power $E_{b\lambda}$ was also developed by Planck in 1901 in conjunction with his famous quantum theory [29, 30] (the credit is largely owed to the Professor Josef Stefan [31] and Professor Ludwig Boltzmann [32]). This relation is known as Planck's law and is expressed as:

$$\begin{aligned} E(\lambda, T) &= \frac{\tau_1}{\lambda^5 \left[\exp\left(\frac{\tau_2}{\lambda T}\right) - 1\right]}, \\ \tau_1 &= 2\pi h \tau_0^2 = 3.742 \times 10^8, \\ \tau_2 &= \frac{h\tau_0}{\kappa} = 1.439 \times 10^4, \end{aligned} \tag{5}$$

where T is the surface temperature of the object in Kelvin (K) and $k = 1.380649 \times 10^{-23}\,\mathrm{J \cdot K^{-1}}$ is the Boltzmann constant.

2.3 Analogy

In this subsection, some concepts are elaborated. The relationship between wavelength λ and pixel $x_{i,j}$ is familiar, as shown in Figure 2. This relationship is calculated by the detector to produce a specific X-ray image. In light of this, we assume that the difference rate of λ corresponds to the difference rate of pixel $x_{i,j}$:

$$d\lambda \propto dx_{i,j}. \tag{6}$$

This assumption is imaginary, which we developed based on our understanding; however, we cannot deny that there is a relationship between the wavelength of X-rays and pixel value of mammogram images. As mentioned previously, a breast tumor has a high density, and therefore it will absorb the photon energy of X radiation. Meanwhile, the wavelength increases because the relationship is inversely proportional (see Equation (3)). This phenomenon is similar to the relationship between photon energy and the pixel values of the X-ray image (see Equation (1)), and thus we can infer the following:

$$\begin{gathered} \because x_{i,j} \propto \frac{1}{E} \text{ and } \lambda \propto \frac{1}{E} \\ \therefore \lambda \approx x_{i,j} \end{gathered} \tag{7}$$

3 METHODOLOGY

3.1 Dataset

The Chinese Mammography Database (CMMD) is public dataset and frequently used for tumor classification and segmentation. The CMMD collection contains breast mammography images and corresponding clinical data. The clinical data for all subjects is stored in The Cancer Imaging Archive under [33]. The imaging data for all subjects is stored in the folder CMMD.

3.2 Computer Specifications and Software

The PC was a ZBook 15 G2, HP, with an Intel(R) Core(TM) i7-4810MQ CPU @ 2.8 GHz, 16 GB of RAM, and an NVIDIA Quadro K1100M GPU. The operating system was Windows 10 Pro 64-bit. The programming language was MATLAB R2020b. All software used in this study was licensed appropriately.

3.3 Proposed Approach

In this section, the detailed steps of the proposed Max Planck architecture are elucidated. The general architecture of the proposed Max Planck algorithm is shown in Figure 3. It contains four proposed parts:

1. first Planck's law operation,
2. second Planck's law operation,
3. the gradient, and
4. the Laplacian operator.

Let the gray mammogram image be expressed in 2D matrix as follows:

$$\mathbf{x} = \begin{bmatrix} x_{11} & x_{12} & \cdots & x_{1N} \\ x_{21} & x_{22} & \cdots & x_{2N} \\ \vdots & \vdots & \ddots & \vdots \\ x_{M1} & x_{M2} & \cdots & x_{MN} \end{bmatrix} = (x_{i,j})_{1 \le i \le M, 1 \le j \le N}. \tag{8}$$

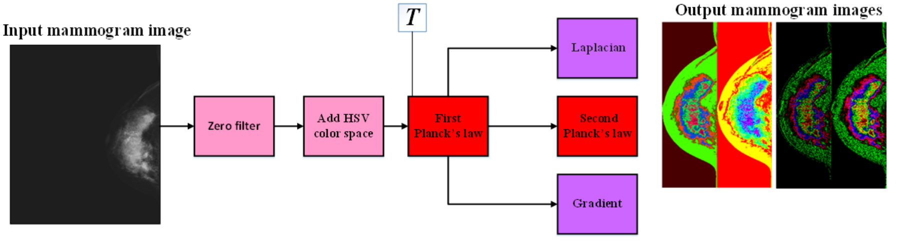

Figure 3. The architecture of the proposed Max Planck algorithm

HSV color space is added to convert the gray mammogram image into a colored image, and the HSV image can be expressed in a 3D matrix as follows:

$$\mathbf{x} = \begin{matrix} \begin{bmatrix} x_{11}^1 & x_{12}^1 & \cdots & x_{1N}^1 \\ x_{21}^1 & x_{22}^1 & \cdots & x_{2N}^1 \\ \vdots & \vdots & \ddots & \vdots \\ x_{M1}^1 & x_{M2}^1 & \cdots & x_{MN}^1 \end{bmatrix} \\ \vdots \\ \begin{bmatrix} x_{11}^Z & x_{12}^Z & \cdots & x_{1N}^Z \\ x_{21}^Z & x_{22}^Z & \cdots & x_{2N}^Z \\ \vdots & \vdots & \ddots & \vdots \\ x_{M1}^Z & x_{M2}^Z & \cdots & x_{MN}^Z \end{bmatrix} \end{matrix} \vdots = (x_{i,j}^k)_{1\le i\le M, 1\le j\le N, 1\le k\le Z}, \tag{9}$$

where $x_{i,j}^k$ is the element (or pixel terms widely used in computer science) of the matrix x, where $i = 1, 2, \ldots, M$; $j = 1, 2, \ldots, N$; $k = 1, 2, \ldots, Z$; M is the number of rows; N is the number of columns; and Z is the number of channels (HSV). At this moment, the mapping operation can be applied. To clarify, each element on matrix x will transfer to the Planck's law function as follow:

$$x_{i,j}^k \mapsto E(x_{i,j}^k, T) = \frac{\tau_1}{(x_{i,j}^k)^5 \left[\exp\left(\frac{\tau_2}{x_{i,j}^k T}\right) - 1\right]}. \tag{10}$$

Now, Planck's law can be applied on matrix x. This operation can be expressed by:

$$E(\mathbf{x}, T) = \frac{\tau_1}{\mathbf{x}^5 \left[\exp\left(\frac{\tau_2}{\mathbf{x}T}\right) - 1\right]}. \tag{11}$$

After we apply Planck's law on matrix x, the gradient and Laplacian operator of Planck's law are executed.

$$\begin{aligned} \nabla E &= \frac{\partial E}{\partial x}\widehat{i} + \frac{\partial E}{\partial y}\widehat{j}, \\ L &= \frac{\Delta E}{4} = \frac{1}{4}\left(\frac{\partial^2 E}{\partial x^2} + \frac{\partial^2 E}{\partial y^2}\right). \end{aligned} \tag{12}$$

3.4 Implementation Details

Table 1 shows the parameters that were considered in the implementation of the proposed Max Planck algorithm. These pivotal parameters were standardized throughout all the experiments.

Speed of light in vacuum	τ_0	2.997×10^8
Planck constant	h	$6.62607015 \times 10^{-34}$
Boltzmann constant	κ	1.380653×10^{-23}
Refractive index of the medium	n	1

Table 1. Experimental Settings

4 EXPERIMENTAL STUDIES

4.1 Results

In this section, we presents our findings. It is obvious that the Max Planck algorithm can enhance images and show more details about the masses in the breast. Furthermore, it can classify each pixel accurately. We changed the value of T from 10^{13} to 10^{16} gradually in order to show what the Max Planck algorithm can detect. We selected one of the most difficult images among the dataset, as shown in Figure 4. Figure 4 a) is the original gray image, while Figure 4 b) is the original HSV image after the color space HSV was added on the original gray mammogram image.

The effect of Planck's law on the mammogram image, as displayed in Figure 5 a), is strong and proves its ability to show the image more clearly with more details; however, this was not our aim. We wanted the Max Planck algorithm to convert all pixels not related to tumors to zero and the tumor shape pixels to become greater than zero. Therefore, Planck's law was repeated. The results of this operation are shown in Figure 5 b). Figure 5 c), and Figure 5 d) is the gradient and Laplacian of the first operation of Planck's law. We did not perform the gradient and Laplacian for the second operation of Planck's law because it completely destroyed the mammogram image. If we compare between Figure 5 a), which is the output image from the first operation of Planck's law, and Figure 5 b), which is the output image from the second operation of Planck's law, Figure 5 b) shows more information about the tumor region. This is one of the benefits of the proposed Max Planck algorithm.

Figures 6, 7, 8, and 9 display the effect of the Max Planck algorithm with a different value of T. We discovered through the experiments that the best value to achieve our purpose was 10^{15}, as shown in Figure 7 a) and Figure 7 b). At that value, the second operation of Planck's law performed much better than the gradient and Laplacian, as displayed in Figure 7 c) and Figure 7 d) specifically.

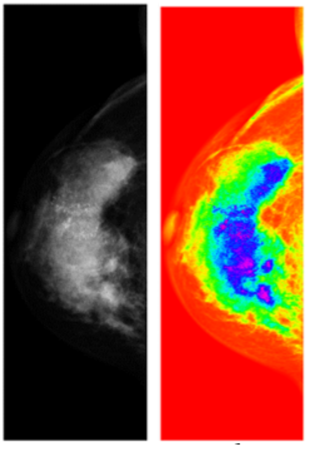

a) Original gray mammogram b) Original HSV mammogram

Figure 4. Images for a breast

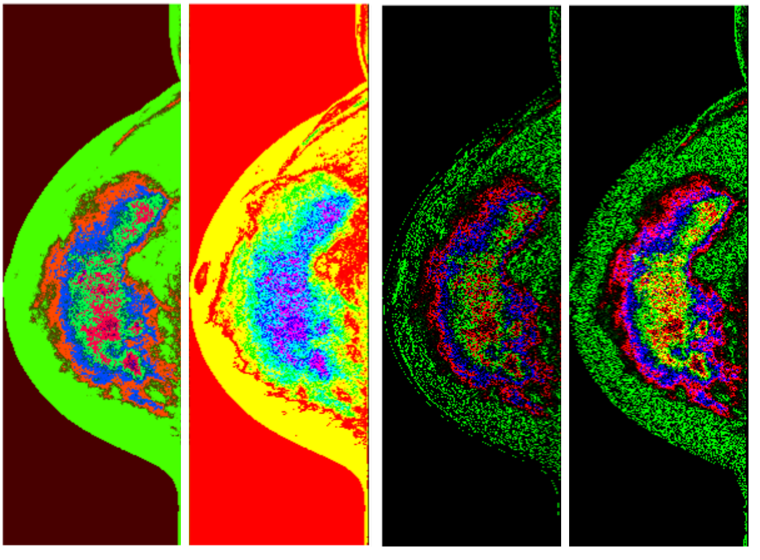

a) b) c) d)

Figure 5. a) Output image from the first operation of Planck's law; b) output image from the second operation of Planck's law; c) the gradient of the first operation of Planck's law; d) the Laplacian operator of the first operation of Planck's law at $T = 10^{13}$

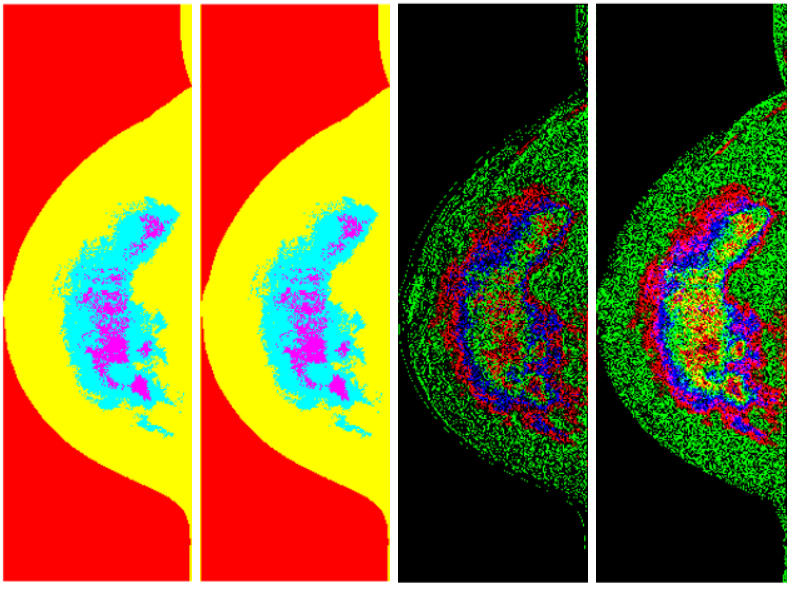

a) b) c) d)

Figure 6. a) Output image from the first operation of Planck's law; b) output image from the second operation of Planck's law; c) the gradient of the first operation of Planck's law; d) the Laplacian operator of the first operation of Planck's law at $T = 10^{14}$

One of the other remarkable advantages of the proposed Max Planck algorithm is that it is stable whatever the value of T is. To clarify, if the value of T is changed to 10^{16} or even ∞, then the output image from the first operation of Planck's law does not change, and thus the output images from the gradient and Laplacian operators also do not change. To support this finding, the output images are shown in Figures 8 a), 8 c), 8 d), 9 a), 9 c), and 9 d).

According to the results, the green color represents the intact cells, and the rest of the colors represent the masses and irregular tissue in the breast. However, the behavior of the tumor, whether benign or malignant, cannot be precisely predicted by using mammogram images alone because the extraction of sample cells or tissues for examination (biopsy) is a decisive factor in determining the presence or extent of the cancer. As we mentioned previously, the purpose of the Max Planck algorithm is to identify the region of masses and irregular tissue clearly and accurately.

4.2 Discussions

To the best of our knowledge, to date, the use of Max Planck's theory for computer vision is undiscovered. These references [20, 21, 22, 23, 24, 25] are provided for the

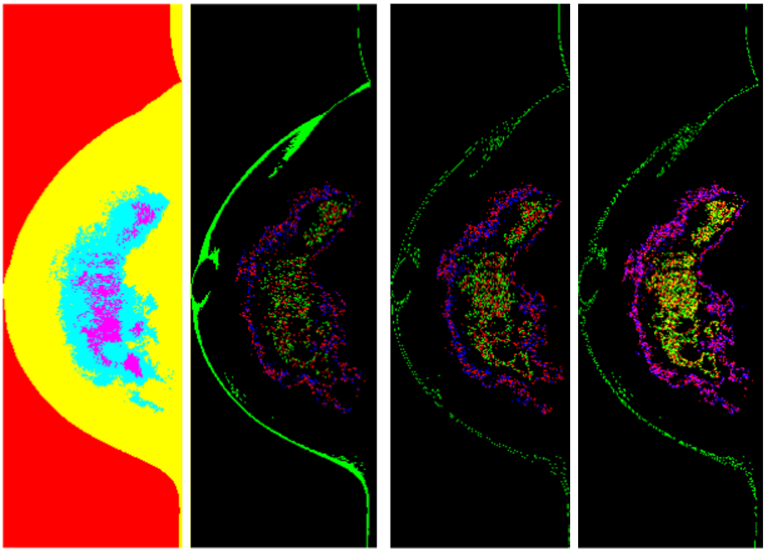

a) b) c) d)

Figure 7. a) Output image from the first operation of Planck's law; b) output image from the second operation of Planck's law; c) the gradient of the first operation of Planck's law; d) the Laplacian operator of the first operation of Planck's law at $T = 10^{15}$

reader's benefit to demonstrate that we are the first to discover the applicability of Max Plank's theory for image segmentation. In this study, we propose a new approach for image segmentation using Planck's law. From the presented findings, Max Planck algorithm can detect abnormality in mammogram images and partition a mammogram image into multiple image segments, also known as image regions or image objects. The aim of our proposed algorithm is to simplify and change the representation of an image into something that is more meaningful and easier to analyze. Moreover, the Max Planck algorithm is able to locate breast masses and boundaries, which helps the radiologist to obtain more information about the tumor's nature.

According to our investigation, there are three classes of segmentation techniques: classical computer vision approaches; more advanced techniques; and deep learning-based techniques. Our proposed method belongs to classical computer vision approaches, and it is a feature detection method for computing abstractions of image information and making local decisions at every image element whether there is an image feature of a given type at that element or not. We demonstrated through experiments that the Max Planck algorithm can detect the class of each pixel. For example, in a mammogram image with many lumps, all the pixels belonging to breast lumps will have a specific color, and its degree depends on the

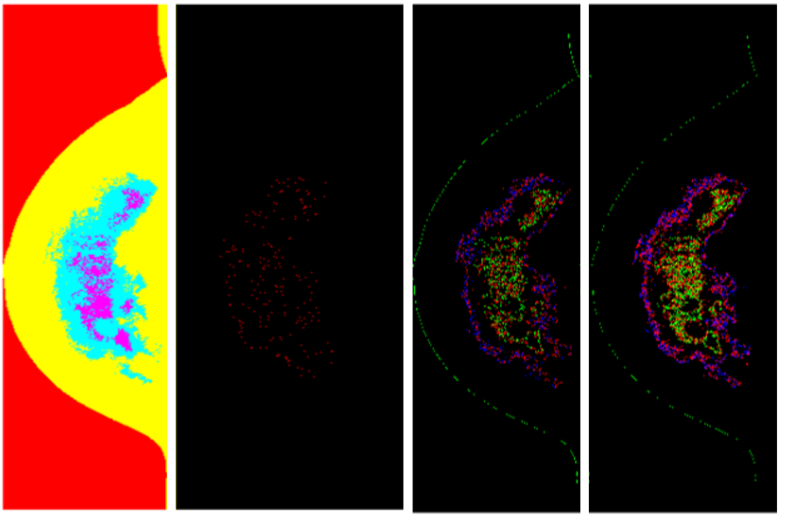

a) b) c) d)

Figure 8. a) Output image from the first operation of Planck's law; b) output image from the second operation of Planck's law; c) the gradient of the first operation of Planck's law; d) the Laplacian operator of the first operation of Planck's law at $T = 10^{16}$

tumor density and the pixels in the intact tissue or normal region will be classified as background and have green color (see Figure 5).

The proposed algorithm cannot classify breast tumors as benign or malignant; nevertheless, our method has the ability to enhance a mammogram image in order to display more information about masses and localize the boundaries of both breast and tumors (see Figure 7). Regarding the deep learning-based segmentation methods, these techniques need many mathematical processes. Indeed, long computational time, risk of missing significant data patterns, a potential drawback of losing background information and foreground texture information, and the negative pixel of the input is simply dropped and can never be reactivated again and potentially resulting in the lost feature information [34, 35]. These serious shortcomings arise due to employing traditional layers such as convolutional layers, nonlinear activation functions layers, batch normalization layers, and polling layers, which would limit their application as a standard medical image segmentation.

A significant advantage of our approach is that it provides greater flexibility as one can change the value of T and quickly obtain many image features. It is important to note that Professor Max Planck used T, and referred to as temperature because he studied the relationship between temperature, wavelength, and photon energy [30]. After that, the famous quantum theory called Planck's law was developed [30]. Based on this theory, we transformed Planck's law from a function of

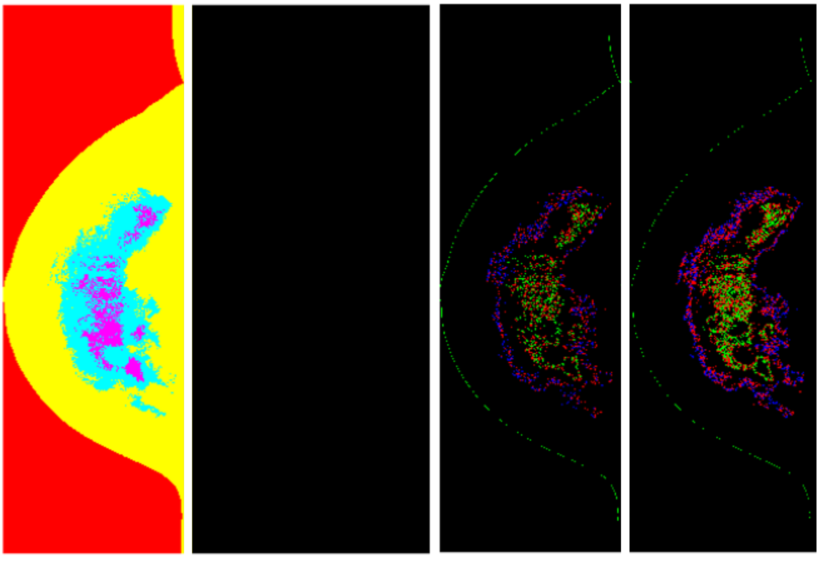

a) b) c) d)

Figure 9. a) Output image from the first operation of Planck's law; b) output image from the second operation of Planck's law; c) the gradient of the first operation of Planck's law; d) the Laplacian operator of the first operation of Planck's law at $T = \infty$

temperature and wavelength into a function of temperature and pixel value. However, in our study, the term 'temperature T' was used as an arbitrary value, and its value was $10^{13} \leq T \leq \infty$. Therefore, we consider this study as an extension of the research conducted by Max Planck's.

5 CONCLUSION

Motivated by the scientist Max Planck who developed Planck's law in 1901, in this study, we created a Max Planck algorithm. This novel algorithm consists of two Planck's law operations, the gradient, and the Laplacian operator. These operations were modified and connected to work together for image segmentation, which is entirely new, not only in the field of digital image processing but also in the field of physics. The conclusions are as follows:

1. By using the analogy concept, we mathematically proved the relationship between the pixel value and wavelength of X-rays. We concluded that pixel value is proportional to wavelength and inversely proportional to photon energy. After that, we replaced the wavelength with the pixel value of the mammogram image. Thus, Planck's law became a function in the temperature and pixel values. No one before us thought or applied this step in physics or in digital image

processing. This step was developed from our understanding and imagining of quantum theory based on Max Planck.

2. By employing Planck's law as an image segmentation algorithm, we obtained brilliant performance, and the proposed algorithm proved its ability to detect the masses regions in breasts accurately and rapidly without the need of a powerful GPU. It can be concluded that the proposed algorithm successfully classifies each pixel in the mammogram image as intact tissue, masses or irregular tissue in the breast. Moreover, the proposed algorithm precisely identifies the edge of the tumor region.
3. Our method is limited to small datasets and is applicable only to grayscale images. It cannot be generalized to all types of data and requires further investigation with different types of images to reach definitive conclusions.

REFERENCES

[1] Roberts, L. G.: Machine Perception of Three-Dimensional Solids. Ph.D. Thesis. Massachusetts Institute of Technology, 1963.

[2] Davis, L. S.: A Survey of Edge Detection Techniques. Computer Graphics and Image Processing, Vol. 4, 1975, No. 3, pp. 248–270, doi: 10.1016/0146-664X(75)90012-X.

[3] Kirsch, R. A.: Computer Determination of the Constituent Structure of Biological Images. Computers and Biomedical Research, Vol. 4, 1971, No. 3, pp. 315–328, doi: 10.1016/0010-4809(71)90034-6.

[4] Marr, D.—Hildreth, E.: Theory of Edge Detection. Proceedings of the Royal Society of London B: Biological Sciences, Vol. 207, 1980, No. 1167, pp. 187–217, doi: 10.1098/rspb.1980.0020.

[5] Canny, J.: A Computational Approach to Edge Detection. IEEE Transactions on Pattern Analysis and Machine Intelligence, Vol. PAMI-8, 1986, No. 6, pp. 679–698, doi: 10.1109/TPAMI.1986.4767851.

[6] Otsu, N.: A Threshold Selection Method from Gray-Level Histograms. IEEE Transactions on Systems, Man, and Cybernetics, Vol. 9, 1979, No. 1, pp. 62–66, doi: 10.1109/TSMC.1979.4310076.

[7] Nock, R.—Nielsen, F.: Statistical Region Merging. IEEE Transactions on Pattern Analysis and Machine Intelligence, Vol. 26, 2004, No. 11, pp. 1452–1458, doi: 10.1109/TPAMI.2004.110.

[8] Dhanachandra, N.—Manglem, K.—Chanu, Y. J.: Image Segmentation Using K-Means Clustering Algorithm and Subtractive Clustering Algorithm. Procedia Computer Science, Vol. 54, 2015, pp. 764–771, doi: 10.1016/j.procs.2015.06.090.

[9] Najman, L.—Schmitt, M.: Watershed of a Continuous Function. Signal Processing, Vol. 38, 1994, No. 1, pp. 99–112, doi: 10.1016/0165-1684(94)90059-0.

[10] Kass, M.—Witkin, A.—Terzopoulos, D.: Snakes: Active Contour Models. International Journal of Computer Vision, Vol. 1, 1988, No. 4, pp. 321–331, doi: 10.1007/BF00133570.

[11] Boykov, Y.—Veksler, O.—Zabih, R.: Fast Approximate Energy Minimization via Graph Cuts. IEEE Transactions on Pattern Analysis and Machine Intelligence, Vol. 23, 2001, No. 11, pp. 1222–1239, doi: 10.1109/34.969114.

[12] Plath, N.—Toussaint, M.—Nakajima, S.: Multi-Class Image Segmentation Using Conditional Random Fields and Global Classification. Proceedings of the 26th Annual International Conference on Machine Learning (ICML '09), 2009, pp. 817–824, doi: 10.1145/1553374.1553479.

[13] Starck, J. L.—Elad, M.—Donoho, D.: Image Decomposition via the Combination of Sparse Representations and a Variational Approach. IEEE Transactions on Image Processing, Vol. 14, 2005, No. 10, pp. 1570–1582, doi: 10.1109/TIP.2005.852206.

[14] Li, Z.—Li, C.—Li, S.—Zhu, S.—Samani, H.: A Sparsity-Based Method for Fault-Tolerant Manipulation of a Redundant Robot. Robotica, Vol. 40, 2022, No. 10, pp. 3396–3414, doi: 10.1017/S0263574722000285.

[15] Minaee, S.—Boykov, Y.—Porikli, F.—Plaza, A.—Kehtarnavaz, N.—Terzopoulos, D.: Image Segmentation Using Deep Learning: A Survey. IEEE Transactions on Pattern Analysis and Machine Intelligence, Vol. 44, 2022, No. 7, pp. 3523–3542, doi: 10.1109/TPAMI.2021.3059968.

[16] Fukushima, K.: Neocognitron: A Self-Organizing Neural Network Model for a Mechanism of Pattern Recognition Unaffected by Shift in Position. Biological Cybernetics, Vol. 36, 1980, No. 4, pp. 193–202, doi: 10.1007/BF00344251.

[17] Zhang, W.—Tanida, J.—Itoh, K.—Ichioka, Y.: Shift-Invariant Pattern Recognition Neural Network and Its Optical Architecture. Proceedings of Annual Conference of the Japan Society of Applied Physics, 1988.

[18] Lecun, Y.—Bottou, L.—Bengio, Y.—Haffner, P.: Gradient-Based Learning Applied to Document Recognition. Proceedings of the IEEE, Vol. 86, 1998, No. 11, pp. 2278–2324, doi: 10.1109/5.726791.

[19] Krizhevsky, A.—Sutskever, I.—Hinton, G. E.: ImageNet Classification with Deep Convolutional Neural Networks. In: Pereira, F., Burges, C. J., Bottou, L., Weinberger, K. Q. (Eds.): Advances in Neural Information Processing Systems 25 (NIPS 2012). Curran Associates, Inc., 2012, pp. 1097–1105, https://proceedings.neurips.cc/paper_files/paper/2012/file/c399862d3b9d6b76c8436e924a68c45b-Paper.pdf.

[20] Acharya, T.—Ray, A. K.: Image Processing: Principles and Applications. John Wiley & Sons, 2005, doi: 10.1002/0471745790.

[21] Gonzales, R. C.—Woods, R. E.: Digital Image Processing. Edition 4th. Pearson Education Limited, 2018.

[22] Pham, D. L.—Xu, C.—Prince, J. L.: Current Methods in Medical Image Segmentation. Annual Review of Biomedical Engineering, Vol. 2, 2000, No. 1, pp. 315–337, doi: 10.1146/annurev.bioeng.2.1.315.

[23] Lee, L. K.—Liew, S. C.—Thong, W. J.: A Review of Image Segmentation Methodologies in Medical Image. In: Sulaiman, H. A., Othman, M. A., Othman, M. F. I., Rahim, Y. A., Pee, N. C. (Eds.): Advanced Computer and Communication Engineering Technology. Springer, Cham, Lecture Notes in Electrical Engineering, Vol. 315, 2015, pp. 1069–1080, doi: 10.1007/978-3-319-07674-4_99.

[24] Rezaei, Z.: A Review on Image-Based Approaches for Breast Cancer Detection, Segmentation, and Classification. Expert Systems with Applications, Vol. 182, 2021, Art. No. 115204, doi: 10.1016/j.eswa.2021.115204.

[25] Ramesh, K. K. D.—Kumar, G. K.—Swapna, K.—Datta, D.—Rajest, S. S.: A Review of Medical Image Segmentation Algorithms. EAI Endorsed Transactions on Pervasive Health and Technology, Vol. 7, 2021, No. 27, Art. No. e6, doi: 10.4108/eai.12-4-2021.169184.

[26] Röntgen, W. C.: On a New Kind of Rays. Science, Vol. 3, 1896, No. 59, pp. 227–231, doi: 10.1126/science.3.59.227.

[27] Dance, D. R.—Christofides, S.—Maidment, A. D. A.—McLean, I. D.—Ng, K. H.: Diagnostic Radiology Physics. International Atomic Energy Agency, 2014.

[28] Huda, W.—Abrahams, R. B.: Radiographic Techniques, Contrast, and Noise in X-Ray Imaging. American Journal of Roentgenology, Vol. 204, 2015, No. 2, pp. W126–W131, doi: 10.2214/AJR.14.13116.

[29] Planck, M.: The Theory of Heat Radiation. P. Blakiston's Son & Co., 1914, `https://www.gutenberg.org/files/40030/40030-pdf.pdf`.

[30] Planck, M.: Ueber das Gesetz der Energieverteilung im Normalspectrum. Annalen der Physik, Vol. 309, 1901, No. 3, pp. 553–563, doi: 10.1002/andp.19013090310 (in German).

[31] Stefan, J.: Über die Beziehung Zwischen der Wärmestrahlung und der Temperatur. Sitzungsberichte der Mathematisch-Naturwissenschaftlichen Classe der Kaiserlichen Akademie der Wissenschaften, Vol. 79, 1879, pp. 391–428, `http://www.ing-buero-ebel.de/strahlung/Original/Stefan1879.pdf`.

[32] Boltzmann, L.: Ableitung des Stefan'schen Gesetzes, Betreffend die Abhängigkeit der Wärmestrahlung von der Temperatur aus der Electromagnetischen Lichttheorie. Annalen der Physik, Vol. 258, 1884, No. 6, pp. 291–294, doi: 10.1002/andp.18842580616 (in German).

[33] Cai, H.—Wang, J.—Dan, T.—Li, J.—Fan, Z.—Yi, W.—Cui, C.—Jiang, X.—Li, L.: An Online Mammography Database with Biopsy Confirmed Types. Scientific Data, Vol. 10, 2023, No. 1, Art. No. 123, doi: 10.1038/s41597-023-02025-1.

[34] Chen, Z.—Ho, P. H.: Global-Connected Network with Generalized ReLU Activation. Pattern Recognition, Vol. 96, 2019, Art. No. 106961, doi: 10.1016/j.patcog.2019.07.006.

[35] Boureau, Y. L.—Ponce, J.—Yann, L.: A Theoretical Analysis of Feature Pooling in Visual Recognition. Proceedings of the 27th International Conference on Machine Learning (ICML 2010), 2010, pp. 111–118, `https://icml.cc/Conferences/2010/papers/638.pdf`.

Yun Zhang received her Bachelor's degree in nursing from the Medical College of Soochow University. She is currently a Clinical Researcher at Gaomi Maternity and Child Healthcare Hospital, where she is responsible for health data science and clinical research management. Her expertise lies in integrating health informatics with clinical practice, utilizing data-driven approaches to enhance patient care, optimizing medical decision-making, and advancing maternal and child healthcare. She has published SCI-indexed research papers and is dedicated to driving innovation in evidence-based healthcare through interdisciplinary collaboration and advanced data analytics.

Refat Mohammed Abdullah Eshaq received his B.Sc. degree in mechanical engineering from the Arab Academy for Science, Technology and Maritime Transport, Alexandria, Egypt, in January 2018, and his M.Sc. degree in mechatronic engineering from the China University of Mining and Technology, Xuzhou, China, in June 2021. His research interests include heat transfer, gas dynamics, fluid mechanics, thermal visual sensing, and deep learning applications in the intelligent industry.

Weian Dong received his Bachelor's degree in mechanical engineering from Zhengzhou University of Aeronautics in 2022 and is currently pursuing his Master's degree in mechanical engineering from the Department of Mechanical Engineering at Hohai University. He is currently researching robotic vision and somatosensory interaction at Hohai University. His research interests include robot vision, deep learning, and human-computer interaction.

Chunxu Li received his Ph.D. degree from Swansea University in 2019 and was appointed as a lecturer at the School of Engineering, Computing and Mathematics, University of Plymouth in January 2020. He has published over 50 academic papers and won the Best Student Paper Award and was shortlisted for the Best Paper Award in IEEE international conferences. He has expertise in ROS, JAVA, C++, Python and MATLAB with over 8 years' working experience on multiple robot platforms, e.g., KUKA iiwa, Baxter, NAO, Universal, etc. He is an Associate Fellow of the Higher Education Academy and a member of IEEE (Institute of Electrical and Electronics Engineers). As the PI and the main co-I, he successfully granted several projects and fundings.